Accepted Manuscript

Synthesis and Antiproliferative Activity of 9-Benzylamino-6-chloro-2-methoxy-acridine Derivatives as Potent DNA-binding Ligands and Topoisomerase II Inhibitors

Wei Zhang, Bin Zhang, Wei Zhang, Ti Yang, Ning Wang, Chunmei Gao, Chunyan Tan, Hongxia Liu, Yuyang Jiang

PII: S0223-5234(16)30248-3

DOI: 10.1016/j.ejmech.2016.03.066

Reference: EJMECH 8491

To appear in: *European Journal of Medicinal Chemistry*

Received Date: 21 December 2015

Revised Date: 11 March 2016

Accepted Date: 25 March 2016

Please cite this article as: W. Zhang, B. Zhang, W. Zhang, T. Yang, N. Wang, C. Gao, C. Tan, H. Liu, Y. Jiang, Synthesis and Antiproliferative Activity of 9-Benzylamino-6-chloro-2-methoxy-acridine Derivatives as Potent DNA-binding Ligands and Topoisomerase II Inhibitors, *European Journal of Medicinal Chemistry* (2016), doi: 10.1016/j.ejmech.2016.03.066.

Synthesis and Antiproliferative Activity of 9-Benzylamino-6-chloro-2-methoxy-acridine Derivatives as Potent DNA-binding Ligands and Topoisomerase II Inhibitors

A series of 9-benzyl acridine derivatives were synthesized and evaluated as good antiproliferative inhibitors. All of them displayed strong Topo II inhibitory activity at 100 μM. The typical compound **8p** showed potent DNA-binding ability, caused DNA double-strand breaks and induced A549 cells apoptosis through caspase-dependent intrinsic pathway.

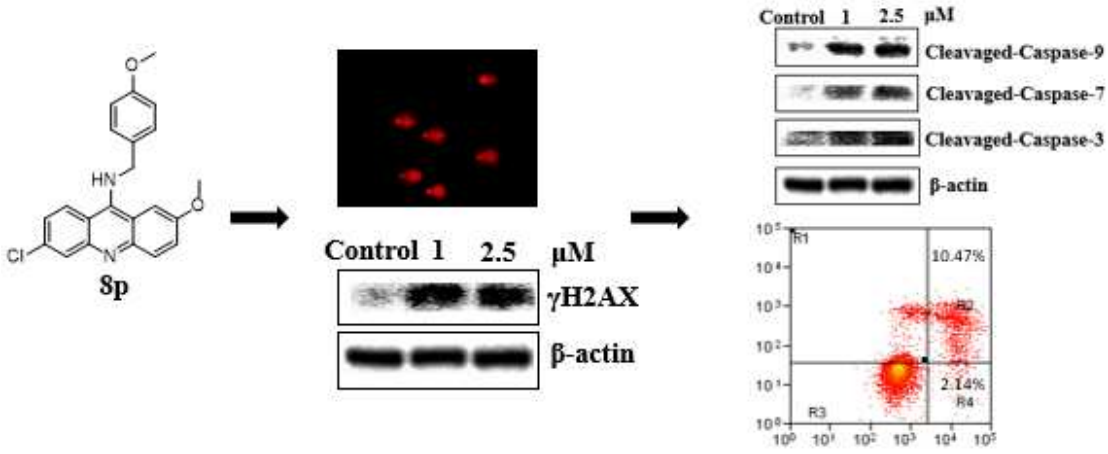

Synthesis and Antiproliferative Activity of 9-Benzylamino-6-chloro-2-methoxy-acridine Derivatives as Potent DNA-binding Ligands and Topoisomerase II Inhibitors

Wei Zhang[a, b, c], Bin Zhang[c], Wei Zhang[b, c], Ti Yang[a], Ning Wang[a, b], Chunmei Gao[a,b*], Chunyan Tan [b, d], Hongxia Liu [b], Yuyang Jiang[a, b, d*]

[a]*Tsinghua University, Department of Chemistry, Beijing 100084, PR China*

[b]*The Ministry-Province Jointly Constructed Base for State Key Lab-Shenzhen Key Laboratory of Chemical Biology, the Graduate School at Shenzhen, Tsinghua University, Shenzhen 518-55, P. R. China*

[c]*ShenzhenAnti-Tumor Drug Development Engineering Laboratory, the Graduate School at Shenzhen, Tsinghua University, Shenzhen 518055, P. R. China*

[d]*Department of Pharmacology and Pharmaceutical Sciences, School of Medicine, Tsinghua University, Beijing, 100084, P. R. China*

Keywords

Acridine derivatives; Topoisomerase II inhibitor; Antiproliferative activity; DNA damage

* Corresponding authors. Tel./Fax: +86 (755) 26032094
e-mail:chunmeigao@sz.tsinghua.edu.cn, jiangyy@sz.tsinghua.edu.cn

Abstract

A series of 9-benzylamino acridine derivatives were synthesized as an extension of our discovery of acridine antitumor agents. Most of these acridine compounds displayed good antiproliferative activity with IC_{50} values in low micromole range and structure-activity relationships were studied. Topo I- and II- mediated relaxation studies suggested that all of our compounds displayed strong Topo II inhibitory activity at 100 μM, while only four exhibited moderate Topo I inhibitory activity. The typical compound **8p** could penetrate A549 cancer cells efficiently. Compound **8p** could intercalate within the double-stranded DNA structure and induce DNA damage. Moreover, compound **8p** could induce A549 cells apoptosis through caspase-dependent intrinsic pathway and arrest A549 cells at the G2/M phase.

1. Introduction

About a century ago, biologists have suggested that there might be a relationship between the pathogenesis of cancer and "specific and abnormal chromosome constitution" [1, 2]. The alterations in DNA structure as well as changes in chromosome structure and number are collectively known as genomic instability, which has been recognized as the most pervasive characteristic of most cancers nowadays [3]. As DNA damages such as single-strand breaks (SSBs), double-strand breaks (DSBs) might lead to cell death, cells possess complex mechanisms to respond to those damages to maintain genomic integrity and cell alive [4]. For the sake of killing cancer cells, both DNA and DNA replication related enzymes can serve as targets for cancer therapy and practiced clinically for decades [3, 5-7]. Among those enzymes, topoisomerases are studied for many years with more prominent effectiveness. Both topoisomerase I (Topo I) and topoisomerase II (Topo II) with the ability to catalyze DNA breakage and religation, facilitate the replication and transcription of DNA, which is essential to mammalian cell division cycle [8, 9]. The following steps were involved in the action of topo enzymes. Firstly, enzymes bind DNA duplex to their DNA-binding and cleavage core, then produce DNA breakage and form a covalent transient DNA-enzyme complex to change the topological structure of DNA. Topo I and Topo II are different here in that Topo I mediates single strand break of a DNA double helix to let another strand across, while Topo II mediates DNA double strand break to pass another noncleaved duplex. At last enzymes get reset after reseal the cleaved DNA backbone [10]. Numerous anticancer drugs used in clinic are those which can interact with DNA and topoisomerases to induce DNA damage and prevent DNA lesion repairment [5, 11]. For example, camptothecin causes SSBs by stabilizing DNA-Topo I-drug complex, etoposide causes DSBs by stabilizing DNA-Topo II-drug complex [12-14].

Acridines (Figure 1, acridine) are firstly used as antibacterial and antiparasite agents with planar aromatic structures that are capable to intercalate into DNA base pairs. Since its anticancer effect has been noticed, considerable researches have been conducted to synthesize more effective and less toxic acridines as anticancer agents [15-17]. Amsacrine (Figure 1, *m*-AMSA) was firstly been proved to interact with Topo II-DNA complex exhibiting clinical efficiency as an antileukaemic agent [15]. For years, *m*-AMSA and its analogues were intensely studied [18, 19]. Most of the

acridine derivatives are focused on the 9-anilino acridine scaffold, paying more attention on the substituents effects in the acridine and anilino rings on the DNA binding ability and cytotoxicity [20-24]. Recently we found that the linkers between acridine and benzene groups affected the bioactivity greatly, among which $-NHCH_2$ was the best. In addition, our work as well as references indicated that acridines with chloro and methoxy groups substituted at C-2 and C-6 positions of acridine ring gave a favorable antiproliferative activity *in vitro* (Figure 1, compound X) [25, 26]. As our continuous efforts for developing new anticancer compounds [26-32], we try to modify the benzyl ring of **3** to generate compounds with more biological activity, since the substitution pattern on the 9-anilinogroup played an important role on the antitumor activity [18, 19, 21, 33-35]. In this work, various 9-benzylamine acridine derivatives (Table 1; **8 (a–w)**) with different substituents in the benzyl group were synthesized for the discovery of potent Topo II targeted anticancer agents and evaluated the structure-activity relationships.

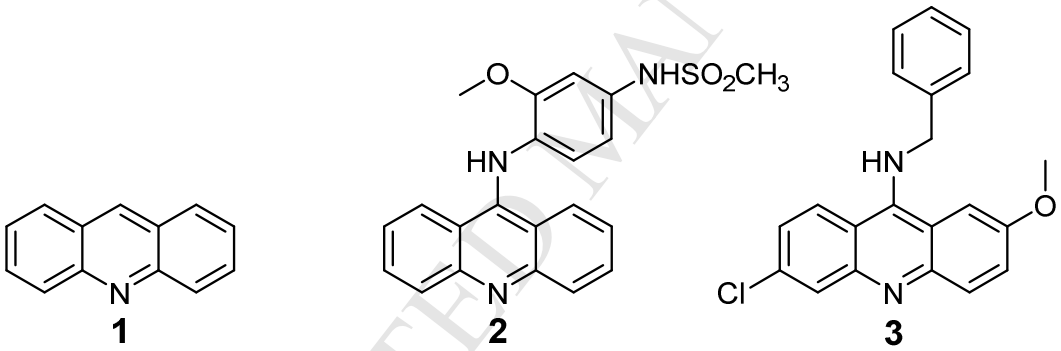

Figure 1. Chemical structures: 1, acridine, 2, *m*-AMSA, 3, compound X.

2. Results and discussion

2.1. Chemistry

Synthesis of the 9-benzylamine acridine derivatives **8 (a-w)** were carried out as shown in Scheme 1 as previously described [25]. Utilizing the Ullmann reaction the anthralic acid **6** was obtained in high yields using Cu as the catalyst refluxed in DMF under basic condition, which was cyclized to the 9-chloroacridine derivative **7**. Reactions of compounds **7** and various substituted benzyl amines were carried out in the presence of a catalytic amount of KI under basic conditions in absolute ethanol to give the desired corresponding **8 (a-w)**.

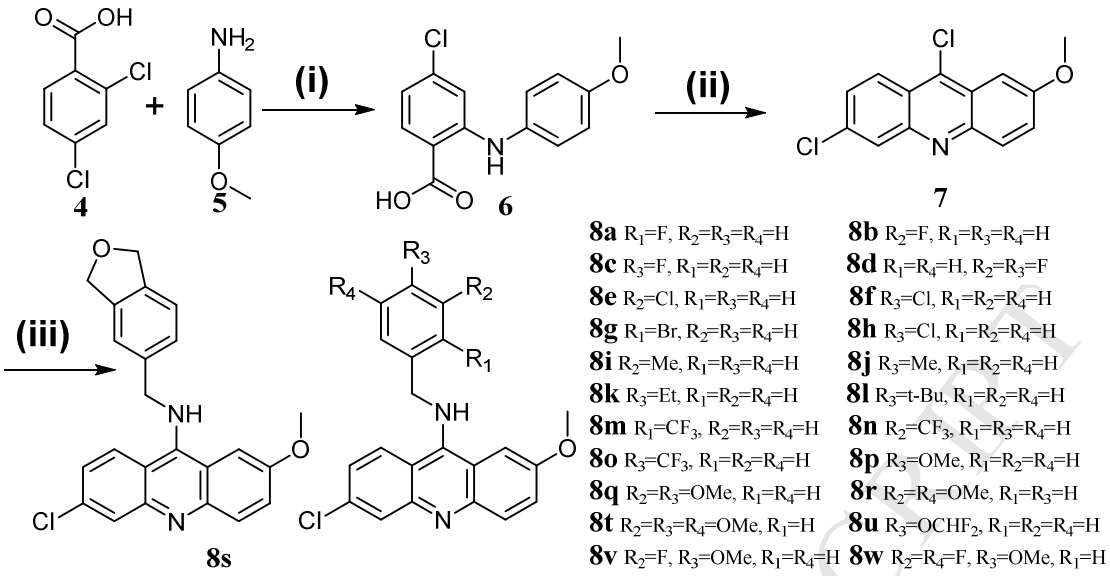

Scheme 1. Reagents and conditions: (i) Cu, K_2CO_3, DMF, reflux; (ii) $POCl_3$, reflux; (iii) various benzyl amines, KI, K_2CO_3, C_2H_5OH, reflux.

2.2. In vitro cytotoxicity

With the chemical library of **8 (a-w)** in hand, the cell proliferation inhibitory activities of all compounds were evaluated using human lung cancer cell line A549, among which, five compounds **8n**, **8p**, **8s**, **8u** and **8v** displayed significant antiproliferative activity with IC_{50} values less than 1 μM (Table 1). As shown from Table 1, although the cytotoxicities typically did not differ more than factor 10, the observed antiproliferative activities were dependent on the nature of the substituents and the substitution pattern on the benzyl ring.

As fluorinated compounds have a remarkable record in medicinal chemistry, compounds **8a-8d** were firstly synthesized to evaluate their antiproliferative activity. The results indicated that the *meta*- or *para*-position is less preferable than *ortho*-position (**8a** vs **8b** and **8c**). To our surprise, the cytotoxicity was lost when both *meta*- and *para*-position were substituted with fluorines (**8d**). The replacement of fluorine by chlorine or bromine resulted in little change in the antiproliferative activity (**8b** vs **8e**, **8c** vs **8f** and **8h**, **8a** vs **8g**).

In addition, alkyl or alkoxyl groups were also played an important role in the activity. The introduction of methyl or ethyl group resulted in a little increase in the antiproliferative activity than the corresponding halogen substituted acridine derivatives (**8i** vs **8b** and **8e**, **8j** and **8k** vs **8c** and **8f**). The replacement of ethyl by

butyl on *para*-position led to a significant decrease of activity (**8l** vs **8k**). The excrescent methoxy(s) was (were) not help to improve the activity (**8p** vs **8q**, **8r**, **8t**), and the replacement of two hydrogens of methoxy group (**8p**) by two fluorines (**8u**) did not change the IC_{50} value so much. Thus we surmised that substituents with higher steric hindrance were not preferred. The replacement of polar methoxy group (**8p**) by methyl (**8j**) / ethyl group (**8k**) or the replacement of trifluoromethyl group (**8n**) by methyl group (**8i**) led to obvious decrease of activities, suggesting that polar substitutions on *meta*- or *para*-position are preferred. What's more, the introduction of fluorine(s) to compound **8p** led to a decrease of activity (**8p** vs **8v** and **8w**). We speculate that the subtle electronic effects might play an important role in the cytotoxicity.

As compounds **8n**, **8p**, **8s**, **8u** and **8v** displayed the best antiproliferative activity against A549 cells, they were selected to test broad-spectrum antitumor activity. Table 2 indicated that the five compounds displayed good antiproliferative activity against the human breast cancer cell line MCF-7, human cervical cancer cell line Hela, human colon cancer cell line HCT-116 and human acute lymphoblastic cancer cell line CCRF-CEM. Compound **8p** displayed the best antiproliferative activity against MCF-7 and Hela cells and good activity against CCRF-CEM cells. While compound **8n** and **8v** exhibited better antiproliferative activity against HCT-116 cells.

Table 1 IC_{50} values of **8 (a-w)** in A549 Cancer Cells.

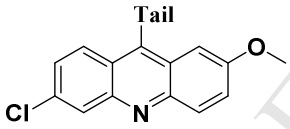

Compd	Tail	C_{50} (μM)	Compd	Tail	IC_{50} (μM)
8a	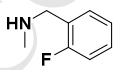	2.82±0.02	8m	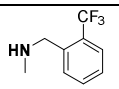	6.32±0.24
8b	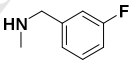	4.19±0.15	8n	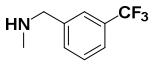	0.16±0.07
8c	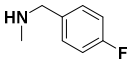	4.05±0.10	8o	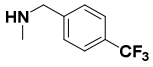	6.04±0.01
8d	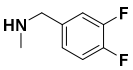	>25	8p	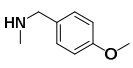	0.61±0.06
8e	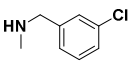	4.64±0.18	8q	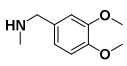	2.56±0.15
8f	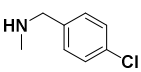	4.20±0.13	8r	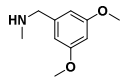	9.20±0.05

8g	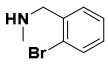	3.00±0.08	8s	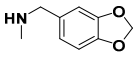	0.65±0.04
8h	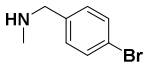	3.26±0.02	8t	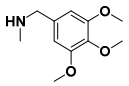	2.18±0.05
8i	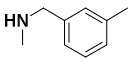	2.22±0.08	8u	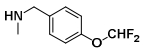	0.72±0.13
8j	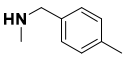	2.63±0.24	8v	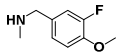	0.95±0.04
8k	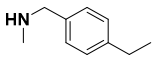	2.58±0.40	8w	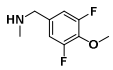	1.82±0.36
8l	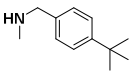	7.03±0.36	Doxorubicin		0.09±0.004
Etoposide		3.82±0.05	Amsacrine		5.96±0.14

Table 2 IC_{50} values of typical compounds in several cancer cell lines.

Compd	Tail	IC_{50} (μM)			
		MCF-7	Hela	HCT-116	CCRF-CEM
8n	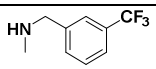	10.50±0.34	10.07±0.43	0.76±0.01	5.11±0.73
8p	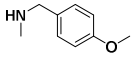	6.95±0.94	1.70±0.26	6.32±0.49	2.54±0.07
8s	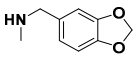	10.33±0.39	7.00±1.68	1.62±0.02	2.00±0.04
8u	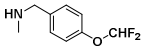	9.95±0.88	4.41±0.24	1.16±0.10	6.87±0.37
8v	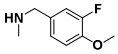	7.60±0.24	4.08±0.31	0.86±0.03	3.08±0.28
Doxorubicin		0.81±0.01	0.78±0.10	0.07±0.03	0.052±0.006
Etoposide		ND	41.21±4.45	6.03±0.70	0.12±0.05
Amsacrine		26.76±0.59	0.34±0.04	0.93±0.21	0.18±0.04

2.3. Topo I and IIα Inhibitory Activities

As the structure of our compounds was similar to that of *m*-AMSA, we anticipate that our compounds might inhibit the activity of topoisomerases. All our newly synthesized compounds were subjected to Topo I and Topo IIα inhibitory assay. Compounds **8c**, **8k**, **8p** and **8q** exhibited apparent Topo I inhibitory activity at 100 μM, further investigation showed that these four compounds also inhibit Topo I

activity at both 75 and 50 μM (Figure 2A). Camptothecin was used as a positive control as Topo I inhibitor. All of our compounds displayed strong Topo IIα inhibitory activity at 100 μM. Amsacrine and etoposide, two well-known DNA intercalating and DNA binding Topo II inhibitors, were used as positive controls. Moreover, studies on five compounds **8n**, **8p**, **8s**, **8u** and **8v** showed that these compounds possessed better Topo IIα inhibitory activities than etoposide at 50 μM and 10 μM (except **8n**) (Figure 2B). This data suggested that most of these acridine compounds served as Topo II specific inhibitors. In addition, compounds **8c**, **8k**, **8p** and **8q** served as both Topo I and Topo II dual inhibitors. Compound **8p** was selected to further investigate the action mechanism due to its better antiproliferative activity against tested tumor cell lines and Topo inhibitory activity.

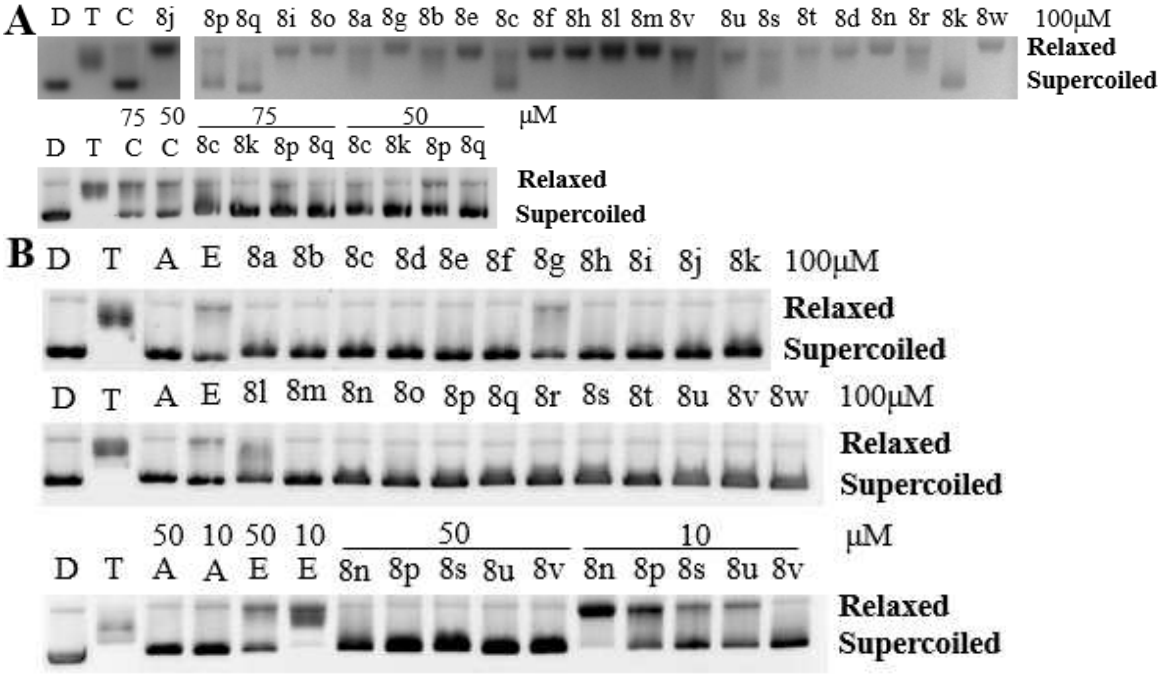

Figure 2. Topo I and Topo IIα inhibitory activities. (A) Topo I: lane D, pBR322 DNA; lane T, Topo I + pBR322 DNA; lane C, camptothecin + Topo I + pBR322 DNA; the others, tested compounds + Topo I + pBR322 DNA. (B) Topo IIα: lane D, pBR322 DNA; lane T, Topo IIα + pBR322 DNA; lane A, amsacrine + Topo IIα + pBR322 DNA; lane E, etoposide + Topo IIα + pBR322 DNA; the others, tested compounds + Topo IIα + pBR322 DNA.

*2.4.Uptake of **8p** in A549cells*

It is important for a designed anticancer drug to penetrate cell membranes to bind to the genomic target with a high efficiency. Therefore, the representative compound **8p**

was subjected to the cellular uptake assay with lung cancer cell line A549 by fluorescence-activated cell sorting. As shown in Figure 3, after A549 cells incubated with compound **8p** for 4 h, as the concentration increased from 1 μM or 5 μM, the fluorescence associated with the cells strongly increased, indicating the ability of **8p** to penetrate cell membranes. In addition, extension incubated time led to no big difference in fluorescence intensity, illustrating that the uptake is up to a maximum after 4 h of incubation.

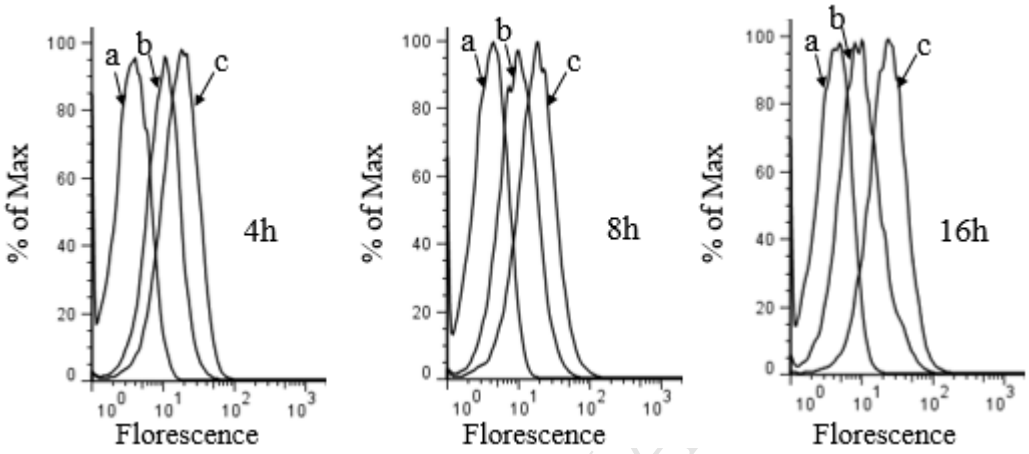

Figure 3. FACS analysis of A549 cancer cells treated with **8p** for 4, 8, 16 h. (a) control, (b) 1 μM, (c) 5 μM.

2.5. DNA interaction studies

As compound **8p** could penetrate cell membranes, it is feasible to study whether the interaction with DNA contributed to its cytotoxicity. UV-visible spectral absorbance was firstly carried out to determine whether compound **8p** could interact with DNA. The results showed that compound **8p** exhibited absorption bands in the region of 365-480 nm (Figure 4A). The maximal absorptions were around 420 nm. When ctDNA was up to 64 μM, the absorption spectra were hypochromicity (60%) and slight bathochromic shifts (10 nm) (Figure 4A), indicating that compound **8p** could intercalate into DNA [36]. The formula (1) was used to calculate the DNA binding constant K_b [37]. The K_b of compound **8p** was 1.68×10^5 M^{-1}, suggesting its good DNA binding capability which was comparable to amsacrine ($K_b = 1.36\times10^5$ M^{-1}, Figure 1s).

$$[DNA]/(\varepsilon_a-\varepsilon_f) = [DNA]/(\varepsilon_b-\varepsilon_f) + 1/K_b(\varepsilon_b-\varepsilon_f) \quad (1)$$

The spectrofluorimetric study was also performed to further evaluate the DNA

binding ability. **8p** (10 μM) exhibited an emission band in the range of 420-750 nm with an excitation wavelength at 400 nm. The fluorescence of **8p** was gradually quenched with increasing concentrations of ctDNA suggesting the interaction between compound **8p** and DNA. The quenching constant K was calculated according to the classical Stern-Volmer Eq. (2) [38]. The quenching constant K of compound **8p** was 1.02×10^5 M^{-1}. Which was in accordance with the absorption spectra. The data indicated that **8p** might intercalate into DNA, since references reported that the intercalation complexes exhibited K from 10^4 to 10^6 M^{-1}, which are conspicuously smaller than the K of groove binders (10^5 -10^9 M^{-1}) [39]. These results indicated that compound **8p** could intercalate within the double-stranded DNA structure and thus might cause DNA damage.

$F_0/F=1+ K[Q]$ (2)

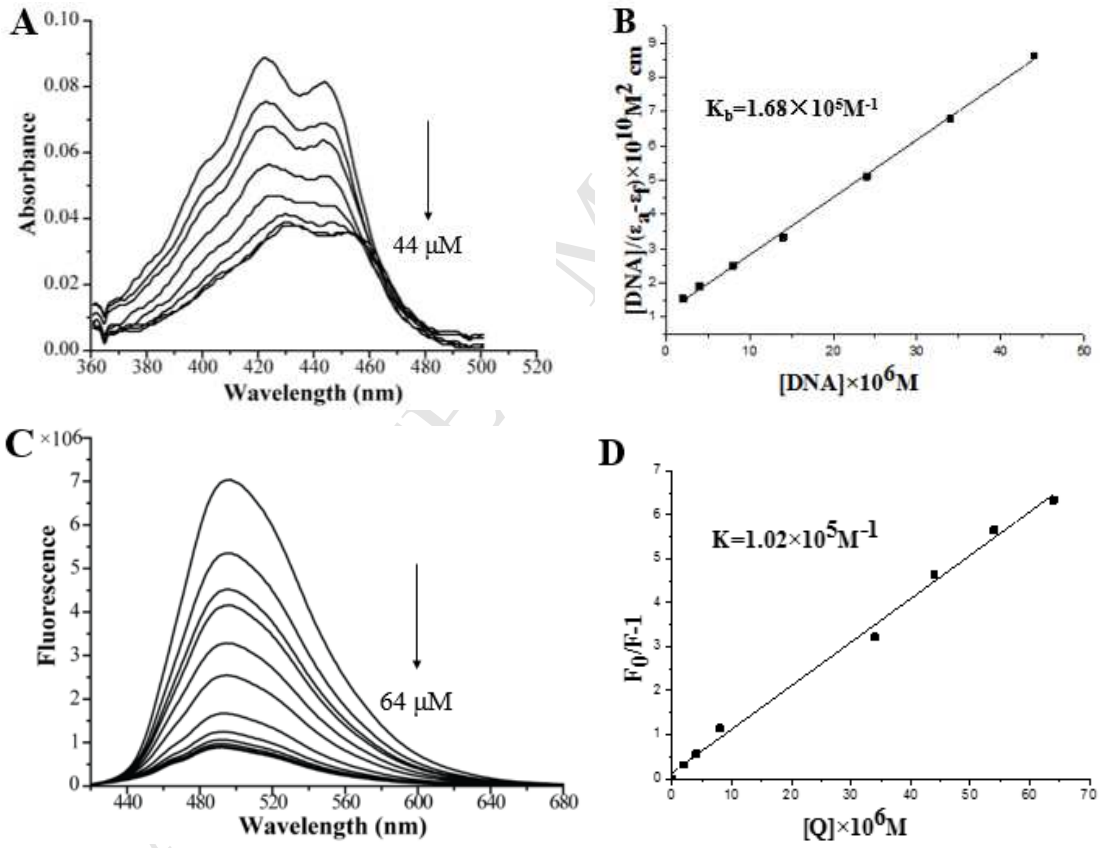

Figure 4. (A) UV-visible absorption spectra of **8p** 10 μM with various concentrations of ctDNA in Tris-HCl buffer (pH 7.4). (B) The plot of absorption data, [DNA], DNA concentration, K_b = 1.68×10^5 M^{-1}. (C) Fluorescence emission spectra of **8p** 10 μM with various concentrations of ctDNA in Tris-HCl buffer (pH 7.4) after excitation at λ_{ex} = 400 nm. (D) The plots of the fluorescence titration, [Q], DNA concentration, K = 1.02×10^5 M^{-1}.

*2.6. DNA damage induced by **8p***

Considering that compounds **8p** functioned as an intercalative catalytic inhibitor, we further investigated the action mode of compound **8p** with A549 cells by observing comet tails in comet assay. As shown in Figure 5A and 5B, untreated control A549 cells had almost no detectable comet tails, while cells displayed significant DNA tails after treatment with compound **8p** at 5 μM, as well as etoposide, the positive control. The results indicated that **8p** could induce severe DNA damage in A549 cells. To gain more insight into the induction of DNA damage of compound **8p**, we monitored the levels of γH2AX in A549 cells treated with **8p**. γH2AX is known as a biomarker for double strand breaks in DNA [40-44]. As shown in Figure 5C, the levels of γH2AX in A549 cells treated **8p** were clearly increased, indicating that compound **8p** caused DSBs.

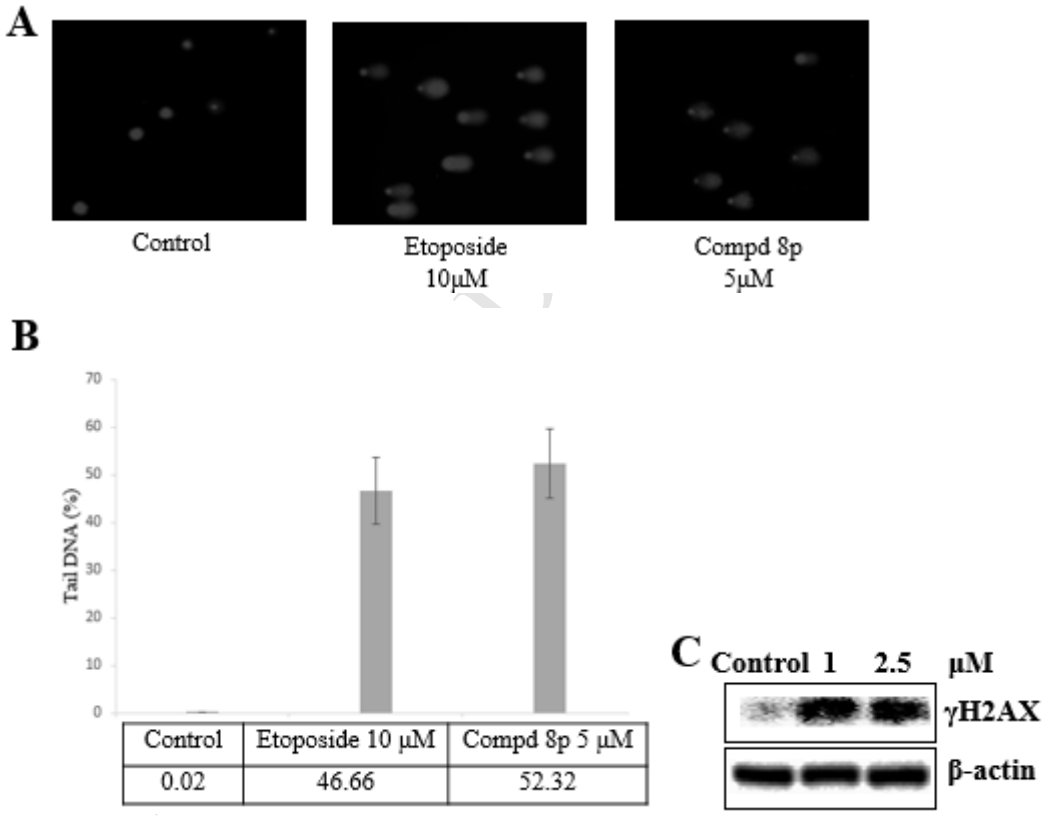

Figure 5. Compound **8p** induce DNA double strands break in A549 cells. (A) Comet assay. Images of A549 cells after treatment with the negative control (nontreated), etoposide, and compound **8p**. (B) Histogram representation of the percentage of tail DNA. (C) **8p** induced the increased expression of γH2AX in A549 cells. Cells were incubated with **8p** at indicated concentrations for 48 h. β-Actin was used as an equal loading control.

*2.7. Apoptosis induced by compound **8p***

Given compound **8p** could cause severe DNA damage, we further investigated the mechanism of compound **8p** inducing A549 cells death using annexin-V (AV)/PI binding assay. In early apoptotic cells, phosphatidyl serine (PS) on cell membrane turned inside-out due to the phospholipid asymmetry lost. As AV possesses a high affinity to PS, AV-FITC could stain early apoptotic cells. While in late apoptotic or necrotic cells, both AV and PI are permeable and stained cells on PS and nucleus, respectively. The results of fluorescence-activated cell sorting analysis performed after treatment of A549 cells with **8p** at the concentrations of 0, 5, 10 μM for 36 or 48 h were shown in Figure 6A. In comparison with the control, A549 cells treated with compounds **8p** exhibited an accumulation of early and late apoptotic cells in a time and dose-dependent manner. For example, the percentage of late apoptotic cells was 0.29% in untreated cells, while it was 10.47% and 88.13% in the cells treated with **8p** at 5, 10 μM for 36 h, respectively. The corresponding percentage was 0.62%, 21.23% and 82.46% in cells treated with **8p** for 48 h, respectively. Also, the percentage of early apoptotic cells showed the same change trend (Figure 6A).

In order to further validate the mechanism of the induction of cellular apoptosis, we monitored the expressions of regulatory proteins related to apoptotic pathway such as cleaved caspase-3, cleaved caspase-7 and cleaved caspase-9 in A549 cells by immunoblotting. Caspase-9 is involved in the mitochondrial pathway. Activated caspase-9 further cleaves downstream caspases including caspase-3 and -7 to initiate the caspase cascade. Caspase-3 and caspase-7 play irreplaceable roles in cell apoptosis once activated by caspase-9 [45]. The activation of caspases is required for the induction and execution of cellular apoptosis [46]. As shown in Figure 6B, the treatment with compound **8p** increased the expression of proapoptotic marker cleaved caspase-9 and caspase-3 and caspase-7. Altogether, our results suggested that compound **8p** was able to induce caspase-dependent intrinsic pathway of apoptosis in A549 cells.

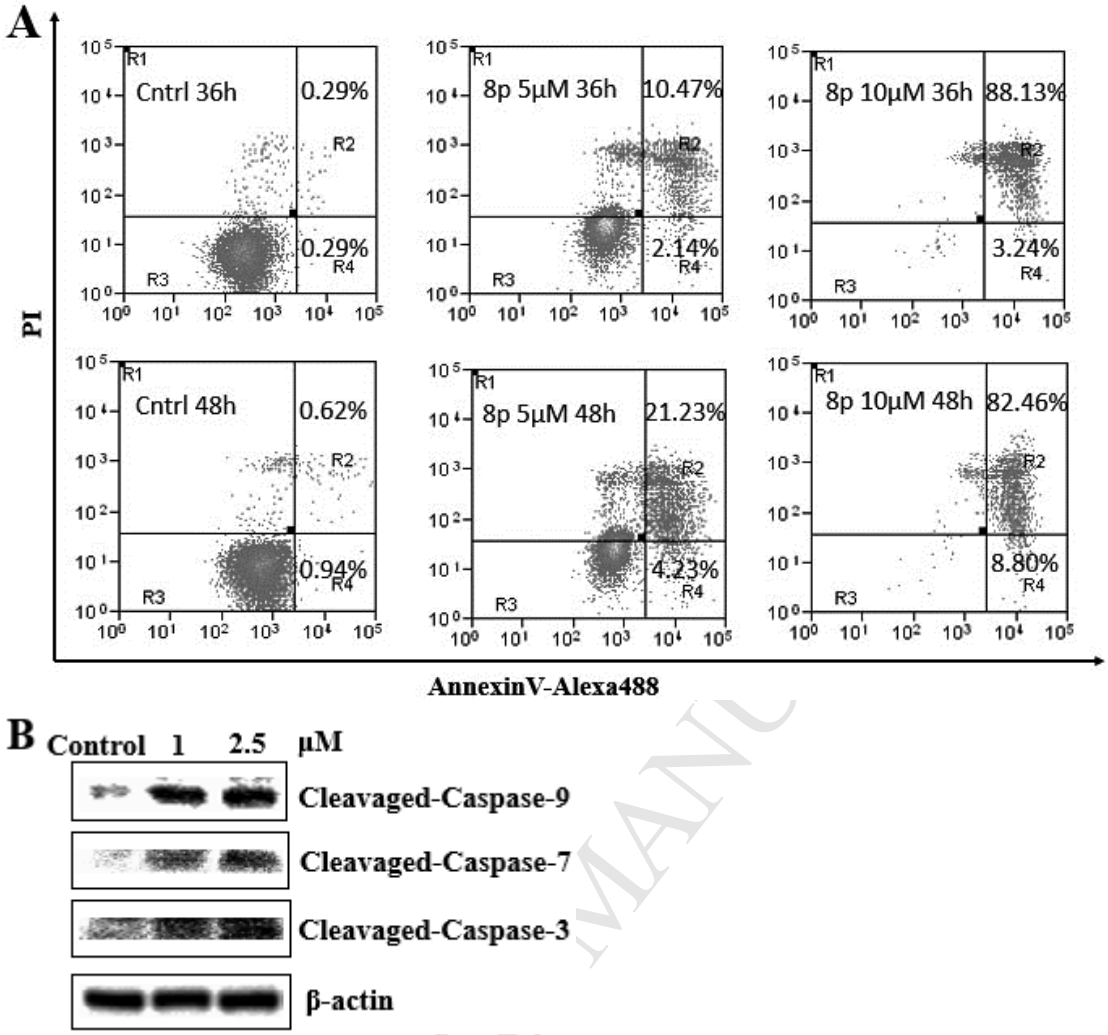

Figure 6. Compound **8p** induced apoptosis in A549 cells. (A) AV/PI assay for the detection of apoptotic A549 cells after treatment with **8p** at the indicated concentrations for 36 or 48 h. (B) Treatment with compound **8p** increased the expression of cleavage-caspase3/7/9 in A549 cells at indicated concentrations after 48 h. β-Actin was used as an equal loading control.

*2.8. G2/M phase arrest induced by **8p***

The cell cycle including four phases G1, S, G2, and M. Cell cycle checkpoints are essential safe guard systems to trigger arrest of cell cycle progression, thus provide time for the cell to correct the dysregulations of cell cycle events before proceeding to the next phase [6, 47, 48]. It is typical for cancer cells that abnormal events such as SSBs, DSBs occur in the cell cycle progression. The cell cycle might be arrested only if the accidental damage corrected. Therefore, we investigated the effect of **8p** on cell cycle distribution of cancer cells using flowcytometry-based total DNA content analysis. After treatment of **8p** at 0.5, 1, and 5 μM in A549 cells for 36 h, as shown in

Figure 7, the cells were arrested in the G2/M phase of the cell cycle in a dose-dependent manner. In response to agents that cause DNA damaging or target cytoskeleton assembly, G2/M checkpoint arrest cells at G2/M phase before entering mitosis [49]. In fact, after 36 h, the cell population in G2/M increases from 7.62% in the untreated cells to 8.12%, 9.62% and 16.52% in the cells treated with **8p** at 0.5, 1, 5 μM, respectively.

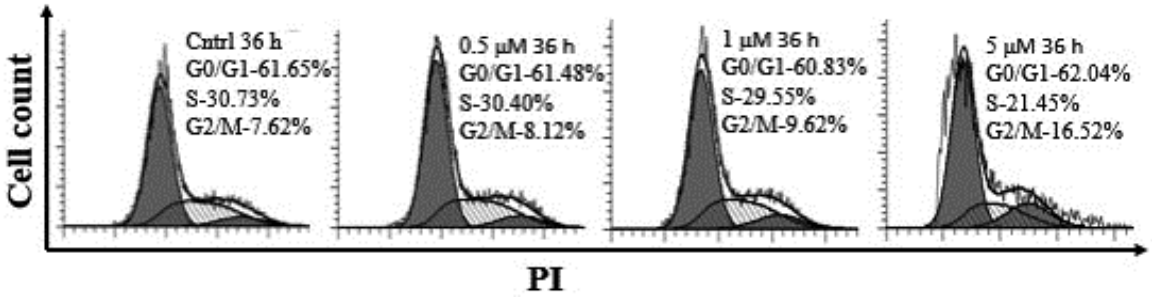

Figure 7. Flowcytometric analysis of compounds **8p** induce G2/M phase arrest in A549 cells. A549 cells were treated with compound **8p** at the indicated concentrations for 36 h.

3. Conclusions

A new series of 9-benzylamine acridine derivatives **8 (a-w)** were simply synthesized and their biological activity were determined. Most of the compounds displayed significant antiproliferative effects against A549 cells. All of our compounds strongly inhibited topo II activity and some of them also exhibited Topo I inhibitory activity. The typical compound **8p** displayed broad antitumor activity, strong DNA binding ability. Further study indicated that compound **8p** significantly induced DNA damage. Compound **8p** arrested cancer cells at G2/M phase and induced them apoptosis potentially by stirring up DNA damage response. The results of this study demonstrated that chemical modification of the 9-benzylamine acridine was a feasible way to develop potent antitumor agents. Further work to optimize the bioactivity is ongoing.

4. Experimental

4.1. Chemistry

Generally, the procedure for the synthesis of **8 (a-w)** was as follows. A mixture of substituted acridine (1) and benzylamine (2 equiv) in ethanol (8 mL) was added potassium carbonate (2 equiv) and potassium iodide (2% equiv). The reaction mixture

was stirred for 30 min at room temperature and refluxed in oil bath for 24-48 h. Then the mixture was extracted with absolute ethanol to give the crude products, which were purified by column chromatography with petroleum ether and ethyl acetate (5:1 v/v).

4.1.1. 6-chloro-N-(2-fluorobenzyl)-2-methoxyacridin-9-amine (8a). Yield 43%; mp 168.6-179.8 °C; ^{1}H NMR (400 MHz, $CDCl_3$) δ 8.09 (s, 1H), 7.99 (dd, *J* = 9.2, 7.6 Hz, 2H), 7.40 (dd, *J* = 9.2, 2.0 Hz, 1H), 7.33-7.26 (m, 3H), 7.18 (d, *J* = 2.4 Hz, 1H), 7.11-7.04 (m, 2H), 4.89 (s, 1H), 4.80 (s, 2H), 3.84 (s, 3H); ^{13}C NMR (101 MHz, $CDCl_3$) δ 162.18, 159.74, 156.52, 148.97, 148.17, 134.81, 131.61, 129.88, 129.85, 129.77, 128.49, 126.23, 126.09, 125.44, 125.03, 124.57, 124.53, 123.63, 119.45, 117.38, 115.76, 115.54, 98.90, 55.37, 48.76, 48.73; HR-MS(ESI): calcd for $C_{21}H_{16}ClFN_2O$ $[M+H]^+$ 367.1013; found: 367.1021.

4.1.2. 6-chloro-N-(3-fluorobenzyl)-2-methoxyacridin-9-amine (8b). Yield 52%; mp 172.4-173.5 °C; ^{1}H NMR (400 MHz, $CDCl_3$) δ 8.09 (d, *J* = 2.0 Hz, 1H), 8.01 (d, *J* = 9.2 Hz, 1H), 7.93 (d, *J* = 9.2 Hz, 1H), 7.41 (dd, *J* = 9.6, 2.8 Hz, 1H), 7.37-7.29 (m, 2H), 7.16 (d, *J* = 7.6 Hz, 2H), 7.11 (d, *J* = 2.4 Hz, 1H), 7.03 (dt, *J* = 7.2, 2.0 Hz, 1H), 4.94 (s, 1H), 4.81 (s, 2H), 3.77 (s, 3H); ^{13}C NMR (101 MHz, $CDCl_3$) δ 164.46, 162.00, 156.41, 149.03, 142.03, 141.96, 134.87, 130.67, 130.59, 125.30, 124.92, 123.53, 122.90, 122.87, 118.58, 116.58, 114.93, 114.73, 114.41, 114.19, 99.00. 55.36, 54.04; HR-MS(ESI): calcd for $C_{21}H_{16}ClFN_2O$ $[M+H]^+$ 367.1013; found: 367.1012.

4.1.3. 6-chloro-N-(4-fluorobenzyl)-2-methoxyacridin-9-amine (8c). Yield 48%; mp 189.2-191.4 °C; ^{1}H NMR (400 MHz, DMSO-d_6) δ 8.29 (d, *J* = 9.2 Hz, 1H), 7.81 (s, 1H), 7.83 (s, 1H), 7.61 (s, 1H), 7.55 (s, 1H), 7.48 (dd, *J* = 8.0, 2.4 Hz, 2H), 7.39 (d, *J* = 8.8, 1H), 7.31-7.26 (m, 1H), 7.20-7.11 (m, 3H), 4.95 (s, 2H), 3.75 (s, 3H); ^{13}C NMR (101 MHz, DMSO-d_6) δ 168.92, 162.25, 159.83, 154.83, 149.97, 135.97, 133.36, 128.62, 128.54, 125.96, 124.12, 122.71, 115.10, 114.89, 104.88, 100.64, 55.16, 51.25, 22.33; HR-MS(ESI): calcd for $C_{21}H_{16}ClFN_2O$ $[M+H]^+$ 367.1013; found: 367.1018.

4.1.4. 6-chloro-N-(3,4-difluorobenzyl)-2-methoxyacridin-9-amine (8d). Yield 63%; mp 205.5-206.4 °C; ^{1}H NMR (400 MHz, DMSO-d_6) δ 8.26 (d, *J* = 9.2 Hz, 1H), 7.86-7.82 (m, 2H), 7.57-7.53 (m, 3H), 7.43-7.38(m, 2H), 7.30 (d, *J* = 6.8 Hz, 2H),

4.94 (s, 2H), 3.78 (s, 3H); ^{13}C NMR (400 MHz, DMSO-d_6) δ 154.90, 150.47, 150.34, 149.86, 149.48, 149.36, 148.03, 147.90, 147.05, 146.93, 133.44, 123.36, 123.33, 117.31, 117.14, 115.83, 115.65, 55.16, 51.15; HR-MS(ESI): calcd for $C_{21}H_{15}ClF_2N_2O$ $[M+H]^+$ 385.0919; found: 385.0927.

4.1.5. 6-chloro-N-(3-chlorobenzyl)-2-methoxyacridin-9-amine (8e). Yield 59%; mp 171.5-171.8 °C; ^{1}H NMR (400 MHz, $CDCl_3$) δ 8.09 (d, *J* = 2.0 Hz, 1H), 8.00 (d, *J* = 9.6 Hz, 1H), 7.92 (d, *J* = 9.2 Hz, 1H), 7.46 (s, 1H), 7.40 (dd, *J* = 9.6, 2.8 Hz, 1H), 7.31-7.28 (m, 3H), 7.25-7.23 (m, 1H), 7.10 (d, *J* = 2.8 Hz, 1H), 4.95 (s, 1H), 4.77 (s, 2H), 3.77 (s, 3H); ^{13}C NMR (101 MHz, $CDCl_3$) δ 156.44, 149.02, 148.22, 147.02, 141.45, 134.98, 134.89, 131.63, 130.29, 128.47, 128.07, 127.48, 125.44, 125.30, 124.96, 123.58, 118.61, 116.59, 98.98, 55.38, 53.98; HR-MS(ESI): calcd for $C_{21}H_{16}Cl_2N_2O$ $[M+H]^+$ 383.0718; found: 383.0708.

4.1.6. 6-chloro-N-(4-chlorobenzyl)-2-methoxyacridin-9-amine (8f). Yield 62%; mp 190.3-192.5 °C; ^{1}H NMR (400 MHz, DMSO-d_6) δ 8.27 (d, *J* = 9.2 Hz, 1H), 7.88 (s, 1H), 7.60 (d, *J* = 7.6 Hz, 1H), 7.54 (s, 1H), 7.48 (d, *J* = 8.0 Hz, 2H), 7.42 – 7.38 (m, 3H), 7.30 (d, *J* = 8.0 Hz, 1H), 4.96 (s, 2H), 3.76 (s, 3H); ^{13}C NMR (101 MHz, DMSO-d_6) δ 154.85, 149.80, 138.99, 133.29, 131.30, 128.53, 128.20, 125.84, 124.27, 122.69, 120.86, 119.07, 116.83, 116.01, 114.52, 104.87, 100.46, 55.16, 51.26; HR-MS(ESI): calcd for $C_{21}H_{16}Cl_2N_2O$ $[M+H]^+$ 383.0718; found: 383.0727.

4.1.7. N-(2-bromobenzyl)-6-chloro-2-methoxyacridin-9-amine (8g). Yield 60%; mp 179.1-180.0 °C; ^{1}H NMR (400 MHz, $CDCl_3$) δ 8.09 (d, *J* = 1.6 Hz, 1H), 7.98 (d, *J* = 9.2 Hz, 2H), 7.59 (dd, *J* = 9.6, 1.6 Hz, 1H), 7.37 (dd, *J* = 9.2, 2.0 Hz, 1H), 7.31 (dd, *J* = 9.2, 2.0 Hz, 1H), 7.24 (dd, *J* = 7.2, 2.0 Hz, 1H), 7.19-7.11 (m, 3H), 5.13 (s, 1H), 4.83 (s, 2H), 3.78 (s, 3H); ^{13}C NMR (101 MHz, $CDCl_3$) δ 156.45, 148.82, 148.16, 147.09, 138.13, 134.79, 133.08, 131.59, 129.89, 129.58, 128.50, 127.92, 125.41, 125.04, 123.74, 123.40, 119.39, 117.34, 98.91, 55.36, 54.66; HR-MS(ESI): calcd for $C_{21}H_{16}BrClN_2O$ $[M+H]^+$ 427.0213; found: 427.0224.

4.1.8. N-(4-bromobenzyl)-6-chloro-2-methoxyacridin-9-amine (8h). Yield 48%; mp 167.3-169.3 °C; ^{1}H NMR (400 MHz, DMSO-d_6) δ 8.26 (d, *J* = 9.6 Hz, 1H), 7.86 (s, 1H), 7.82 (d, *J* = 6.8 Hz, 1H), 7.56-7.38 (m, 6H), 7.29 (d, *J* = 8.4 Hz, 1H), 4.94 (s,

2H), 3.76 (s, 3H); ^{13}C NMR (101 MHz, DMSO-d_6) δ 171.73, 154.86, 149.85, 139.41, 133.34, 131.51, 131.27, 131.12, 130.88, 129.25, 128.91, 128.43, 125.96, 122.63, 119.78, 55.17, 51.38, 20.82; HR-MS(ESI): calcd for $C_{21}H_{16}BrClN_2O$ $[M+H]^+$ 427.0213; found: 427.0211.

4.1.9. 6-chloro-2-methoxy-N-(3-methylbenzyl)acridin-9-amine (8i). Yield 68%; mp 161.1-161.5 °C; ^{1}H NMR (400 MHz, $CDCl_3$) δ 8.09 (d, *J* = 2.0 Hz, 1H), 8.01 (d, *J* = 9.6 Hz, 1H), 7.96 (d, *J* = 9.2 Hz, 1H), 7.41 (dd, *J* = 9.2, 2.4 Hz, 1H), 7.31 – 7.26 (m, 2H), 7.22 – 7.14 (m, 4H), 4.93 (s, 1H), 4.80 (s, 2H), 3.78 (s, 3H), 2.35 (s, 3H); ^{13}C NMR (101 MHz, $CDCl_3$) δ 156.21, 149.52, 148.41, 147.16, 139.34, 138.84, 134.81, 131.70, 128.99, 128.71, 128.52, 128.21, 124.98, 124.80, 124.51, 123.82, 118.33, 116.34, 99.26, 55.38, 54.78, 21.42; HR-MS(ESI): calcd for $C_{22}H_{19}ClN_2O$ $[M+H]^+$ 363.1264; found: 363.1265.

4.1.10. 6-chloro-2-methoxy-N-(4-methylbenzyl)acridin-9-amine (8j). Yield 79%; mp 170.6-171.8 °C; ^{1}H NMR (400 MHz, DMSO-d_6) δ 8.30 (d, *J* = 9.6 Hz, 1H), 7.87 (s, 1H), 7.82 (d, *J* = 8.8 Hz, 1H), 7.59 (d, *J* = 1.6 Hz, 2H), 7.38 (d, *J* = 8.4 Hz, 1H), 7.33 (d, *J* = 8 Hz, 2H), 7.27 (d, *J* = 9.2 Hz, 1H), 7.15 (d, *J* = 8 Hz, 2H), 4.93 (s, 2H), 3.75 (s, 3H); ^{13}C NMR (101 MHz, DMSO-d_6) δ 154.90, 150.07, 136.85, 135.96, 133.30, 130.70, 128.93, 127.12, 126.64, 124.16, 122.68, 114.46, 100.69, 55.28, 51.62, 20.55; HR-MS(ESI): calcd for $C_{22}H_{19}ClN_2O$ $[M+H]^+$ 363.1264; found: 363.1265.

4.1.11. 6-chloro-N-(4-ethylbenzyl)-2-methoxyacridin-9-amine (8k). Yield 55%; mp 104.8-105.9 °C; ^{1}H NMR (400 MHz, DMSO-d_6) δ 8.32 (d, *J* = 7.6 Hz, 1H), 7.87 (s, 1H), 7.82 (d, *J* = 8.0 Hz, 1H), 7.57 (s, 1H), 7.39-7.35 (m, 3H), 7.28 (d, *J* = 8.8 Hz, 1H), 7.18 (d, *J* = 8.0 Hz, 2H), 4.93 (s, 2H), 2.57 (q, *J* = 7.6 Hz, 2H), 1.14 (t, *J* = 7.6 Hz, 3H); ^{13}C NMR (400 MHz, DMSO-d_6) δ 154.80, 150.08, 142.33, 137.11, 133.25, 130.56, 127.65, 126.63, 125.95, 124.05, 122.56, 116.77, 114.50, 100.79, 55.14, 55.10, 51.78, 27.60, 15.39; HR-MS(ESI): calcd for $C_{23}H_{21}ClN_2O$ $[M+H]^+$ 377.1421; found: 377.1415.

4.1.12. N-(4-(tert-butyl)benzyl)-6-chloro-2-methoxyacridin-9-amine (8l). Yield 69%; mp 143.5-145.1 °C; ^{1}H NMR (400 MHz, DMSO-d_6) δ 8.35 (d, *J* = 9.6 Hz, 1H), 7.85 (d, *J* = 2.0 Hz, 1H), 7.83 (d, *J* = 9.2 Hz, 1H), 7.57-7.54 (m, 2H), 7.40-7.37 (m, 4H),

7.31 (dd, *J* = 2.8 Hz, 2H), 4.92 (d, *J* = 7.2 Hz 2H), 3.68 (s, 3H). ^{13}C NMR (400 MHz, DMSO-d_6) δ 154.74, 150.10, 149.26, 147.84, 146.18, 136.84, 133.18, 130.63, 127.07, 126.33, 125.80, 124.99, 124.12, 122.68, 116.68, 114.47, 100.71, 55.01, 51.59, 33.97, 30.93; HR-MS(ESI): calcd for $C_{25}H_{25}ClN_2O$ $[M+H]^+$ 405.1734; found: 405.1741.

4.1.13. 6-chloro-2-methoxy-N-(2-(trifluoromethyl)benzyl)acridin-9-amine (8m). Yield 5%; mp 195.8-196.9 °C; ^{1}H NMR (400 MHz, DMSO-d_6) δ 8.16 (d, *J* = 9.2 Hz, 1H), 8.09 (d, *J* = 8.0 Hz, 1H), 7.88-7.77 (m, 3H), 7.60-7.56 (m, 2H), 7.42-7.40 (m, 2H), 7.30 (d, *J* = 9.2 Hz, 1H), 5.09 (s, 2H), 3.60 (s, 3H). ^{13}C NMR (400 MHz, DMSO-d_6) δ 154.93, 149.85, 149.26, 146.16, 136.84, 132.82, 130.80, 129.32, 128.30, 127.66, 127.23,125.24, 124.31, 123.04,114.42,100.12,54.76, 48.77,28.78; HR-MS(ESI): calcd for $C_{22}H_{16}ClF_3N_2O$ $[M+H]^+$ 417.0982; found: 417.0970.

4.1.14. 6-chloro-2-methoxy-N-(3-(trifluoromethyl)benzyl)acridin-9-amine (8n). Yield 53%; mp 116.7-118.4 °C; ^{1}H NMR (400 MHz, DMSO-d_6) δ 8.30 (d, *J* = 9.2 Hz, 1H), 7.89 (s, 1H), 7.87 (s, 1H), 7.81 (d, *J* = 9.2 Hz 1H), 7.75 (d, *J* = 7.2Hz, 1H), 7.65-7.57 (m, 3H), 7.51 (d, *J* = 2Hz, 1H), 7.39 (dd, *J* = 9.2, 2.4 Hz, 1H), 7.32 (d, *J* = 7.6 Hz, 1H), 5.05 (s, 2H), 3.72 (s, 3H); ^{13}C NMR (400 MHz, DMSO-d_6) δ 154.89, 150.10, 141.61, 133.53, 130.83, 129.41, 129.28, 129.12, 128.80, 125.99, 125.40, 124.00, 123.52, 123.39, 123.35, 122.69, 55.03, 51.76; HR-MS(ESI): calcd for $C_{22}H_{16}ClF_3N_2O$ $[M+H]^+$ 417.0982; found: 417.0987.

4.1.15. 6-chloro-2-methoxy-N-(4-(trifluoromethyl)benzyl)acridin-9-amine (8o). Yield 42%; mp 141.3-142.7 °C; ^{1}H NMR (400 MHz, CDCl3) δ 8.09 (s, 1H), 8.00 (d, J = 9.6 Hz, 1H), 7.90 (d, J = 9.2 Hz, 1H), 7.63 (d, J = 8.4 Hz, 2H), 7.52 (d, J = 8.0 Hz, 2H), 7.40 (dd, J = 9.2, 2.4 Hz, 1H), 7.28 (dd, J = 9.6, 2.0 Hz, 1H), 7.26 (s, 1H)， 7.08 (d, J = 2.4 Hz, 1H), 4.97 (s, 1H), 4.85 (s, 2H), 3.74 (s, 3H); ^{13}C NMR (101 MHz, CDCl3) δ 156.47, 148.96, 148.19, 143.43, 134.94, 130.75, 130.43, 130.10, 129.78, 127.59, 126.01, 125.98, 125.94, 125.90, 125.37, 124.94, 123.47, 122.67, 118.62, 116.58, 98.98, 55.32, 53.99; HR-MS(ESI): calcd for $C_{22}H_{16}ClF_3N_2O$ $[M+H]^+$ 417.0981; found: 417.0986.

4.1.16. 6-chloro-2-methoxy-N-(4-methoxybenzyl)acridin-9-amine (8p). Yield 65%;

mp 156.6-157.7 °C; ^{1}H NMR (400 MHz, DMSO-d_6) δ 8.31 (d, J = 9.2 Hz, 1H), 7.86 (s, 1H), 7.81 (d, J = 9.2 Hz, 1H), 7.60 (s, 1H), 7.39 (d, J = 9.6 Hz, 1H), 7.35 (d, J = 8.0 Hz, 2H), 7.28 (d, J = 9.2 Hz, 1H), 7.35 (d, J = 8.0 Hz, 2H), 6.90 (d, J = 8.0 Hz, 2H), 4.90 (s, 2H), 3.77 (s, 3H), 3.71 (s, 3H); ^{13}C NMR (101 MHz, DMSO-d_6) δ 158.25, 154.91, 150.15, 147.71, 133.38, 131.73, 130.45, 127.94, 126.81, 126.21, 124.11, 122.61, 116.98, 114.61, 113.80, 100.93, 55.33, 54.95; 51.49; HR-MS(ESI): calcd for $C_{22}H_{19}ClN_2O_2$ $[M+H]^+$ 379.1213; found: 379.1205.

4.1.17. 6-chloro-N-(3,4-dimethoxybenzyl)-2-methoxyacridin-9-amine (8q). Yield 61%; mp 159.8-160.4 °C; ^{1}H NMR (400 MHz, DMSO-d_6) δ 8.34 (d, J = 9.6 Hz, 1H), 7.86 (s, 1H), 7.82 (d, J = 9.2 Hz, 1H), 7.62 (d, J = 1.6 Hz, 1H), 7.39 (dd, J =9.2, 2.0 Hz, 1H), 7.30 (d, J = 7.6 Hz, 1H), 7.04 (s, 1H), 6.934-6.875 (m, 2H), 4.89 (s, 2H), 3.78 (s, 3H), 3.70 (s, 3H), 3.67 (s, 3H); ^{13}C NMR (101 MHz, DMSO-d_6) δ 154.82, 150.18, 148.55, 147.63, 133.29, 132.14, 130.42, 129.42, 126.84, 126.10, 124.11, 122.63, 118.63, 114.58, 111.57, 110.59, 100.63, 55.29, 55.20; 55.16; 51.69; HR-MS(ESI): calcd for $C_{23}H_{21}ClN_2O_3$ $[M+H]^+$ 409.1319; found: 409.1314.

4.1.18. 6-chloro-N-(3,5-dimethoxybenzyl)-2-methoxyacridin-9-amine (8r). Yield 79%; mp 147.9-149.5 °C; ^{1}H NMR (400 MHz, DMSO-d_6) δ 8.31 (d, J = 9.2 Hz, 1H), 7.86 (s, 1H), 7.81 (d, J = 9.2 Hz, 1H), 7.60 (d, J = 2.4 Hz, 1H), 7.40 (dd, J = 9.2, 2.8 Hz,1H), 7.31 (dd, J = 9.2, 2.0 Hz, 1H), 6.63 (s, 2H), 6.39 (t, J = 2.0 Hz, 1H), 4.90 (s, 2H), 3.76 (s, 3H), 3.69 (s, 6H); ^{13}C NMR (400 MHz, DMSO-d_6) δ 160.45, 154.82, 150.29, 142.40, 133.48, 126.05, 124.05, 122.61, 116.81, 114.43, 104.57, 101.05, 98.56, 55.38, 55.15, 54.91, 51.94; HR-MS(ESI): calcd for $C_{23}H_{21}ClN_2O_3$ $[M+H]^+$ 409.1319; found: 409.1328.

4.1.19. N-(benzo[d][1,3]dioxol-5-ylmethyl)-6-chloro-2-methoxyacridin-9-amine (8s). Yield 44%; mp 158.6-160.4 °C; ^{1}H NMR (400 MHz, DMSO-d_6) δ 8.30 (d, J = 9.6 Hz, 1H), 7.86 (s, 1H), 7.81 (d, J = 9.6 Hz, 1H), 7.60 (d, J = 2.4 Hz,1H), 7.40 (dd, J = 9.2, 2.4 Hz, 1H), 7.30 (dd, J = 9.2, 2.0 Hz, 1H), 7.00 (s, 1H),6.92-6.86 (m, 2H), 4.88 (s, 2H),3.80 (s, 3H). ^{13}C NMR (400 MHz, DMSO-d_6) δ 154.85, 150.17, 147.22, 146.02, 133.57, 133.50, 129.50, 126.16, 124.06, 122.57, 119.75, 116.85, 114.42, 107.95, 107.14, 101.05, 100.69, 100.71, 55.25, 51.69; HR-MS(ESI): calcd for $C_{22}H_{17}ClN_2O_3$ $[M+H]^+$ 393.1006; found: 393.1008.

4.1.20. 6-chloro-2-methoxy-N-(3,4,5-trimethoxybenzyl)acridin-9-amine (8t). Yield 27%; mp 200.7-202.3 °C; ^{1}H NMR (400 MHz, DMSO-d_6) δ 8.35 (d, J = 9.2 Hz, 1H), 7.88 (s, 1H), 7.82 (d, J = 9.2 Hz, 1H), 7.59 (d, J = 2.4 Hz ,1H), 7.40 (dd, J = 9.6, 2.4 Hz, 1H), 7.34 (dd, J = 9.2, 2.0 Hz, 1H), 6.77 (s, 2H), 4.89 (s, 2H), 3.75 (s, 3H) , 3.69 (s, 6H) , 3.63 (s, 3H). ^{13}C NMR (400 MHz, DMSO-d_6) δ 154.94, 152.86, 150.53, 136.30, 135.79, 133.52, 126.19, 124.21, 122.89, 117.22, 114.93, 104.03, 100.99, 59.92, 55.71, 55.21, 52.47; HR-MS(ESI): calcd for $C_{24}H_{23}ClN_2O_4$ $[M+H]^+$ 439.1425; found: 439.1423.

4.1.21. 6-chloro-N-(4-(difluoromethoxy)benzyl)-2-methoxyacridin-9-amine (8u). Yield 10%; mp 121.8-123.1 °C; ^{1}H NMR (400 MHz, DMSO-d_6) δ 8.31 (d, J = 9.2 Hz, 1H), 7.86 (s, 1H), 7.81 (d, J = 9.2 Hz, 1H), 7.57 (d, J = 2 Hz, 1H), 7.51 (d, J = 8.4, 2H), 7.43-7.02 (m,4H), 4.99 (s, 2H), 3.75 (s, 3H). ^{13}C NMR (400 MHz, DMSO-d_6) δ 154.88, 150.46, 149.70, 146.98, 136.63, 133.79, 128.26, 126.17, 125.80, 124.19, 122.66, 118.38, 116.84, 116.08, 114.27, 113.52, 100.12, 55.20, 51.27; HR-MS(ESI): calcd for $C_{22}H_{17}ClF_2N_2O_2$ $[M+H]^+$ 415.1025; found: 415.1019.

4.1.22. 6-chloro-N-(3-fluoro-4-methoxybenzyl)-2-methoxyacridin-9-amine (8v). Yield 71%; mp 145.4-147.2 °C; ^{1}H NMR (400 MHz, DMSO-d_6) δ 8.29 (d, J = 9.2 Hz, 1H), 7.89 (s, 1H), 7.84 (d, J = 9.6 Hz, 1H), 7.57 (s, 1H), 7.51 (s, 1H), 7.40 (d, J = 8.4 Hz, 1H), 7.30 (dd, J = 12.6,1.6 Hz 1H), 7.18 (d, J = 8.8 Hz, 1H), 7.12 (t, J = 8.4 Hz, 1H), 4.89 (s, 2H), 3.79 (s, 3H), 3.78 (s, 3H). ^{13}C NMR (400 MHz, DMSO-d_6) δ 154.88, 152.45, 150.02, 149.95, 145.90, 145.80, 133.37, 132.81, 126.05, 123.99, 122.75, 122.72, 117.08, 114.67, 114.39, 114.21, 113.66, 100.82, 55.80, 55.20, 51.12; HR-MS(ESI): calcd for $C_{22}H_{18}ClFN_2O_2$ $[M+H]^+$ 397.1119; found: 397.1109.

4.1.23. 6-chloro-N-(3,5-difluoro-4-methoxybenzyl)-2-methoxyacridin-9-amine (8w). Yield 81%; mp 195.2-196.9 °C; ^{1}H NMR (400 MHz, CDCl3) δ 8.11 (s, 1H), 8.03 (d, J = 9.2 Hz, 1H), 7.92 (d, J = 9.2 Hz, 1H), 7.43 (dd, J = 9.2, 2.4 Hz, 1H), 7.34 (dd, J = 9.2, 2.0 Hz, 1H), 7.12 (s, 1H), 7.00 (d, J = 4.8 Hz, 1H), 4.73 (s, 2H), 4.01 (s, 3H), 3.84 (s, 3H); ^{13}C NMR (400 MHz, CDCl3) δ 157.25, 157.19, 156.60, 154.77, 154.70, 148.75, 135.01, 134.62, 125.51, 124.96, 123.46, 118.73, 116.67, 111.18, 111.11, 111.01, 110.95, 99.87, 61.90, 55.44, 55.43, 29.72; HR-MS(ESI): calcd for

$C_{22}H_{17}ClF_2N_2O_2$ $[M+H]^+$ 415.1025; found: 415.1024.

4.2. Cell Proliferation Assay

Cell proliferation assays based on MTT were performed with 6 cancer cell lines. Briefly, cells were seeded in 96-well plates at a density of 4-8 × 10^3 cells per well with incubation overnight in a 5% CO_2 incubator at 37 °C, the growth medium in each well was then exchanged with 0.1 mL of fresh medium containing graded concentrations of compounds to be tested or equal DMSO and incubated continuously for 48 h. Then 10 μL MTT solution (5 mg/mL) was added to each well, and the cells were incubated for additional 4 h. The MTT-formazan crystals were dissolved in 100 μL of DMSO, the absorbance of each well was measured at 490 nm using anautomatic ELISA reader system (TECAN, CHE). Etoposide and Doxorubicin were used as positive controls.

4.3. Human Topo I and Topo IIα relaxation Assay

The inhibition of compounds to Topoisomerases I and Topo IIα were determined by assessing the relaxation of supercoiled pBR322 plasmid DNA. The assay was performed in a final volume of 20 μL reaction volume containing 500 ng of supercoiled DNA pBR322 (Takara Biotechnology, Japan) and 1 unit of human Topo I (Takara Biotechnology, Japan) or Topo IIα (USB Corp., USA) with or without our compounds in the reaction buffer. The reaction mixtures were incubated at 37 °C for 10-15 min and terminated by adding 4 μL of DNA loading buffer. Electrophoresis was performed on a 0.8% agarose gel at 80 V for 30 min in TAE buffer. Then stained gels for 10 min with ethidium bromide (2.5 μg/mL) and destain in water for 5 min. DNA bands were visualized with UV light. Camptothecin (Sigma, USA) was used as a positive control as topo I inhibitor and etoposide (Sigma, USA) were used as a Topo II inhibitor, respectively.

4.4. Absorption spectra

Compound 8p was diluted into Tris-HCl buffer (pH 7.4) to a final concentration of 10 μM and then ctDNA was added with concentration of 0-44 μM. After 5 min

standing the solution was subjected to UV-vis absorption spectra measurement on a Beckman Coulter DU 800 spectrophotometer.

4.5. Fluorescence emission spectra

Compounds 8p was diluted to a final concentration of 10 μM in Tris-HCl buffer (10 mM, pH 7.4), followed adding ctDNA into the system. The final concentration of ctDNA was ranged from 0 to 64 μM. Fluorescence mission spectra were determined on Fluorolog spectrometer with Xenon arc lamp used as excitation light source. The emission spectra were detected from 420-750 nm with an excitation wavelength of 400 nm.

4.6. FACS Analysis

For uptake studies, the cells have been treated for 4 h with 8p (1 and 5 μM). After incubation, the cells were trypsinized and pelleted. The pellets were resuspended in 200 μL of PBS and immediately analyzed by FACS. A minimum of 10000 cells for each sample were acquired and analyzed with an excited wavelength of 400 nm.

For cell cycle Analysis, approximately 2×10^5 cells per well were seeded in six-well plate and incubated for 12 h in serum-free medium following treated with graded concentrations of compounds for 24 h. Cells were harvested by trypsinization, then fixed in ice-cold absolute methanol. Cells were stained with 4 μg/mL PI and 0.1 mg/mL RNaseA in PBS. After incubated in the dark at room temperature for 30 min, simples were subjected to flowcytometric analysis.

For Annexin V-propidium iodide assay, A549 cells were seeded in a six-well plates in a density of 2×10^5 cells per well, incubated overnight and then treated with graded concentrations of compounds for 24 h. Cellular apoptosis was determined by annexin V-PI apoptosis detection kit (Beyotime, CN) following its instructions. Cells in early or late apoptotic phases were represented as cumulative percentage compared with control.

4.7. Comet Assay

Approximately 10^5 A549 cells per well were seeded in a 6-well plate with

incubation for 12 h. Cells were then treated with etoposide or compounds for 24 h in serum free media and DMSO group was set as control. The collected cells were resuspended in ice-cold PBS at a density of 10^5/mL. 7 μL of the prepared cells were mixed with 70 μL of low-melting agarose at 37 °C and spread on coagulated normal-melting agarose, then covered with low-melting agarose after it was coagulated. Then the slides were submerged in lysis buffer for 2 h followed in the alkaline solution for 0.5 h at 4 °C. Electrophoresis was performed at 300 mA in alkaline solution for 25 min in dark. Slides were neutralized thrice with Tris-HCl buffer then stained with PI for 10 min in dark at 4 °C. Comet images were captured with a fluorescent microscope microscope (Olympus, Japan). A total of 50 A549 cells were randomly selected for statistical analysis. The results were represented in the extent of DNA damage.

4.8. Western Blot Assay

A549 cells were grown on 60 mm plates at 1×10^6 cells until reaching 80% confluency. The cells were then treated with graded concentration of compounds to be tested and incubated for 48 h and harvested by trypsinization. Collected Cells were lysed in lysis buffer solution containing 50 mM Tris-HCl, 300 mM NaCl, 1% Triton X-100, 10% glycerol, 1.5 mM $MgCl_2$, 1 mM $CaCl_2$, 1 mM PMSF, and 1% protease inhibitor cocktail. Then 40 μg of protein per sample was resolved by 12 or 15% SDS-PAGE and transferred to a PVDF membrane (Millipore, USA). The membranes were blocked with 5% skim milk in Tris buffered saline containing 0.1% Tween 20 (TBST) and probed with primary antibodies in a dilution ratio of 1:1000 for 6-8 h. The blots were washed, exposed to HRP-conjugated anti rabbit IgG (Cell Signaling Technology Inc. USA) in a dilution ratio of 1:2000 for 2 h, and detected with ECL Western blotting detection reagent (Animal Genetics Inc., Korea). All primary antibodies used were purchased from Cell Signaling Technology Inc. (USA). Western blot images were taken by LAS-3000 (Fuji Photo Film Co., Ltd., Japan) and analyzed using Multi-Gauge Software (Fuji Photo Film Co. Ltd., Japan).

Acknowledgments

The authors would like to thank the financial supports from Shenzhen Municipal Development and Reform Commission (Disciplinary Development Program for Chemical Biology), the Chinese National Natural Science Foundation (21272134 and 21372141), and Shenzhen Sci& Tech Bureau (JCYJ20130402164027386, JCYJ20150331151358131, CXZZ20150529165045064, and CXB201104210014A).

Conflict of Interest The authors declare no conflicts of interest.

Appendix A. Supplementary material

NMR spectrum and high resolution mass spectrometry can be found in supplementary material online.

References

[1] T. Boveri, G. Fischer, Jena, Zur frage der entstehung maligner tumoren, Science 40 (1914) 857-859.

[2] H. Harris, Concerning the origin of malignant tumours by Theodor Boveri. Translated and annotated by Henry Harris. Preface, J. Cell. Sci. 121 Suppl 1 (2008) 1-84.

[3] C.J. Lord, A. Ashworth, The DNA damage response and cancer therapy, Nature 481 (2012) 287-294.

[4] A. Ciccia, S.J. Elledge, The DNA Damage Response: Making It Safe to Play with Knives, Mol. Cell 40 (2010) 179-204.

[5] N. Hosoya, K. Miyagawa, Targeting DNA damage response in cancer therapy, Cancer Sci. 105 (2014) 370-388.

[6] S. Solier, Y.W. Zhang, A. Ballestrero, Y. Pommier, G. Zoppoli, DNA damage response pathways and cell cycle checkpoints in colorectal cancer: current concepts and future perspectives for targeted treatment, Curr. Cancer Drug Targets 12 (2012) 356-371.

[7] T. Helleday, E. Petermann, C. Lundin, B. Hodgson, R.A. Sharma, DNA repair pathways as targets for cancer therapy, Nat. Rev. Cancer 8 (2008) 193-204.

[8] J.L. Nitiss, Targeting DNA topoisomerase II in cancer chemotherapy, Nat. Rev. Cancer 9 (2009) 338-350.

[9] J.L. Nitiss, DNA topoisomerase II and its growing repertoire of biological functions, Nat. Rev. Cancer 9 (2009) 327-337.

[10] J.J. Champoux, DNA topoisomerases: Structure, function, and mechanism, Annu. Rev. Biochem. 70 (2001) 369-413.

[11] A.K. McClendon, N. Osheroff, DNA topoisomerase II, genotoxicity, and cancer, Mutat. Res. 623 (2007) 83-97.

[12] S.H. Chen, N.L. Chan, T.S. Hsieh, New Mechanistic and Functional Insights into DNA Topoisomerases, Annu. Rev. Biochem. 82 (2013) 139-170.

[13] S.M. Vos, E.M. Tretter, B.H. Schmidt, J.M. Berger, All tangled up: how cells direct, manage and exploit topoisomerase function, Nat. Rev. Mol. Cell Bio. 12 (2011) 827-841.

[14] A.J. Schoeffler, J.M. Berger, DNA topoisomerases: harnessing and constraining energy to govern chromosome topology, Q. Rev. Biophys. 41 (2008) 41-101.

[15] W.A. Denny, Tumor-activated prodrugs - A new approach to cancer therapy, Cancer Invest. 22 (2004) 604-619.

[16] G. Cholewinski, K. Dzierzbicka, A.M. Kolodziejczyk, Natural and synthetic acridines/acridones as antitumor agents: their biological activities and methods of synthesis, Pharmacol Rep. 63 (2011) 305-336.

[17] M. Kukowska-Kaszuba, K. Dzierzbicka, Synthesis and structure-activity studies of peptide-acridine/acridone conjugates, Curr. Med. Chem. 14 (2007) 3079-3104.

[18] P. Belmont, J. Bosson, T. Godet, M. Tiano, Acridine and acridone derivatives, anticancer properties and synthetic methods: where are we now?, Anti-Cancer Agents. Med. Chem. 7 (2007) 139-169.

[19] B. Zhang, X. Li, B. Li, C. Gao, Y. Jiang, Acridine and its derivatives: a patent review (2009 - 2013), Expert. Opin. Ther. Pat. 24 (2014) 647-664.

[20] M.R. Galdino-Pitta, M.G.R. Pitta, M.C.A. Lima, S.L. Galdino, I.R. Pitta, Niche for Acridine Derivatives in Anticancer Therapy, Mini-Rev. Med. Chem. 13 (2013) 1256-1271.

[21] P. Belmont, I. Dorange, Acridine/acridone: a simple scaffold with a wide range of application in oncology, Expert. Opin. Ther. Pat. 18 (2008) 1211-1224.

[22] J. Kaur, P. Singh, Acridine derivatives: a patent review (2009 - 2010), Expert. Opin. Ther. Pat. 21 (2011) 437-454.

[23] B.C. May, J. Witkop, J. Sherrill, M.O. Anderson, P.B. Madrid, J.A. Zorn, S.B. Prusiner, F.E. Cohen, R.K. Guy, Structure-activity relationship study of 9-aminoacridine compounds in scrapie-infected neuroblastoma cells, Bioorg. Med. Chem. Lett. 16 (2006) 4913-4916.

[24] M. Oxoby, F. Moreau, L. Durant, A. Denis, J.M. Genevard, V. Vongsouthi, S. Escaich, V. Gerusz, Towards Gram-positive antivirulence drugs: new inhibitors of Streptococcus agalactiae Stk1, Bioorg. Med. Chem. Lett. 20 (2010) 3486-3490.

[25] X. Luan, C. Gao, N. Zhang, Y. Chen, Q. Sun, C. Tan, H. Liu, Y. Jin, Y. Jiang, Exploration of acridine scaffold as a potentially interesting scaffold for discovering novel multi-target VEGFR-2 and Src kinase inhibitors, Bioorg. Med. Chem. 19 (2011) 3312-3319.

[26] X. Lang, L. Li, Y. Chen, Q. Sun, Q. Wu, F. Liu, C. Tan, H. Liu, C. Gao, Y. Jiang, Novel synthetic acridine derivatives as potent DNA-binding and apoptosis-inducing antitumor agents, Bioorg. Med. Chem. 21 (2013) 4170-4177.

[27] J. Lin, X. Jin, Y. Bu, D. Cao, N. Zhang, S. Li, Q. Sun, C. Tan, C. Gao, Y. Jiang, Efficient synthesis of RITA and its analogues: derivation of analogues with improved antiproliferative activity via modulation of p53/miR-34a pathway, Org. Biomol. Chem. 10 (2012) 9734-9746.

[28] F. Jin, D. Gao, Q. Wu, F. Liu, Y. Chen, C. Tan, Y. Jiang, Exploration of N-(2-aminoethyl)piperidine-4-carboxamide as a potential scaffold for development of VEGFR-2, ERK-2 and Abl-1 multikinase inhibitor, Bioorg. Med. Chem. 21 (2013) 5694-5706.

[29] F. Jin, D. Gao, C. Zhang, F. Liu, B. Chu, Y. Chen, Y.Z. Chen, C. Tan, Y. Jiang, Exploration of 1-(3-chloro-4-(4-oxo-4H-chromen-2-yl)phenyl)-3-phenylurea derivatives as selective dual inhibitors of Raf1 and JNK1 kinases for anti-tumor treatment, Bioorg. Med. Chem. 21 (2013) 824-831.

[30] C. Gao, B. Li, B. Zhang, Q. Sun, L. Li, X. Li, C. Chen, C. Tan, H. Liu, Y. Jiang, Synthesis and biological evaluation of benzimidazole acridine derivatives as potential DNA-binding and apoptosis-inducing agents, Bioorg. Med. Chem. 23 (2015) 1800-1807.

[31] X. Li, C. Gao, T. Yang, B. Zhang, C. Tan, H. Liu, Y. Jiang, A POCl3-mediated synthesis of substituted fused azoacridones derivatives, RSC Adv. 5 (2015) 28670-28678.

[32] B. Zhang, K. Chen, N. Wang, C. Gao, Q. Sun, L. Li, Y. Chen, C. Tan, H. Liu, Y. Jiang, Molecular design, synthesis and biological research of novel pyridyl acridones as potent DNA-binding and apoptosis-inducing agents, Eur. J. Med. Chem. 93 (2015) 214-226.

[33] S.M.M. de Almeida, E.A. Lafayette, L.P.B.G. da Silva, C.A.D. Amorim, T.B. de Oliveira, A.L.T.G. Ruiz, J.E. de Carvalho, R.O. de Moura, E.I.C. Beltrao, M.D.A. de Lima, L.B. de Carvalho, Synthesis, DNA Binding, and Antiproliferative Activity of Novel Acridine-Thiosemicarbazone Derivatives, Int. J. Mol. Sci. 16 (2015) 13023-13042.

[34] J. Janockova, J. Plsikova, J. Kasparkova, V. Brabec, R. Jendzelovsky, J. Mikes, J. Koval, S. Hamulakova, P. Fedorocko, K. Kuca, M. Kozurkova, Inhibition of DNA topoisomerases I and II and growth inhibition of HL-60 cells by novel acridine-based compounds, Eur. J. Pharm. Sci. 76 (2015) 192-202.

[35] G.C. Muscia, G.Y. Buldain, S.E. Asis, Design, synthesis and evaluation of acridine and fused-quinoline derivatives as potential anti-tuberculosis agents, Eur. J. Med. Chem. 73 (2014) 243-249.

[36] R. Martinez, L. Chacon-Garcia, The search of DNA-intercalators as antitumoral drugs: what it worked and what did not work, Curr. Med. Chem. 12 (2005) 127-151.

[37] H.F. Wang, R. Shen, N. Tang, Synthesis and characterization of the Zn(II) and Cu(II) piperidinyl isoeuxanthone complexes: DNA-binding and cytotoxic activity, Eur. J. Med. Chem. 44 (2009) 4509-4515.

[38] Y.J. Hu, Y. Liu, X.S. Shen, X.Y. Fang, S.S. Qu, Studies on the interaction between 1-hexylcarbamoyl-5-fluorouracil and bovine serum albumin, J. Mol. Struct. 738 (2005) 143-147.

[39] H. Ihmels, D. Otto, Intercalation of organic dye molecules into double-stranded DNA general principles and recent developments, Top. Curr. Chem. 258 (2005) 161-204.

[40] W.M. Bonner, C.E. Redon, J.S. Dickey, A.J. Nakamura, O.A. Sedelnikova, S. Solier, Y. Pommier, OPINION gamma H2AX and cancer, Nat. Rev. Cancer 8 (2008) 957-967.

[41] A. Ivashkevich, C.E. Redon, A.J. Nakamura, R.F. Martin, O.A. Martin, Use of the gamma-H2AX assay to monitor DNA damage and repair in cancer research, Cancer lett. 327 (2012) 123-133.

[42] A.M. Algotar, A.E. Cress, R.B. Nagle, D. Drinkwitz, N.S. Lodhia, P.A. Thompson, S.P. Stratton, DNA damage and repair markers (H2AX and RAD51) improve accuracy of prostate cancer diagnosis and improve identification of aggressive disease, Cancer Res. 74 (2014).

[43] C.R. Lu, M. Xiong, Y. Luo, J. Li, Y.J. Zhang, Y.Q. Dong, Y.J. Zhu, T.H. Niu, Z. Wang, L.N. Duan, Genome-wide transcriptional analysis of apoptosis-related genes and pathways regulated by H2AX in lung cancer A549 cells, Apoptosis 18 (2013) 1039-1047.

[44] E.P. Rogakou, W. Nieves-Neira, C. Boon, Y. Pommier, W.M. Bonner, Initiation of DNA fragmentation during apoptosis induces phosphorylation of H2AX histone at serine 139, J. Biol. Chem. 275 (2000) 9390-9395.

[45] N.A. Thornberry, Y. Lazebnik, Caspases: Enemies within, Science 281 (1998) 1312-1316.

[46] N.A. Thornberry, Caspases: key mediators of apoptosis, Chem. Biol. 5 (1998) R97-R103.

[47] M.B. Kastan, J. Bartek, Cell-cycle checkpoints and cancer, Nature 432 (2004) 316-323.

[48] Y. Dai, S. Grant, Methods to study cancer therapeutic drugs that target cell cycle checkpoints, Methods Mol. Biol. 782 (2011) 257-304.

[49] J.A. Choi, J.Y. Kim, J.Y. Lee, C.M. Kang, H.J. Kwon, Y.D. Yoo, T.W. Kim, Y.S. Lee, S.J. Lee, Induction of cell cycle arrest and apoptosis in human breast cancer cells by quercetin, Int. J. Oncol. 19 (2001) 837-844.

- A series of 9-benzylamine acridines were synthesized.
- The *in vitro* cytotoxic effects in cancer cells were evaluated.
- All the compounds displayed good topoisomerase II inhibition activity.
- Compound **8p** acted as a potent DNA-binding Ligand and topoisomerase II inhibitor.
- Compound **8p** induced a potent apoptotic response in A549 lung cancer cells.
- Compound **8p** arrested A549 lung cancer cells at the G2/M-phase.